

The solid solution structure of $\text{BiSr}_x\text{Ca}_{1-x}\text{O}_{2.50}$

GUOHONG XIONG, MINQUAN WANG, XIANPING FAN

Department of Materials Science and Engineering, Zhejiang University, Hangzhou 310027, People's Republic of China

GUANGLIE LU

The Center Laboratory, Hangzhou University, Hangzhou 310028, People's Republic of China

The formation and solid-solution structure of $\text{BiSr}_x\text{Ca}_{1-x}\text{O}_{2.50}$ were studied by X-ray powder diffraction analysis, and the crystallography data of the phase are given. The crystal structure of $\text{BiSr}_x\text{Ca}_{1-x}\text{O}_{2.50}$ belongs to the monoclinic system with space group $P1m1$ or $P12/m1$, and the cell parameters for $\text{BiCaO}_{2.50}$ ($x=0.00$) are $a=1.8363$ nm, $b=0.5366$ nm, $c=1.4670$ nm and $\beta=100.26^\circ$. $\text{BiSr}_x\text{Ca}_{1-x}\text{O}_{2.50}$ is a solid solution of Bi–Ca–O and Bi–Sr–O. When the strontium solid solubility $\text{Sr}/\text{Sr}+\text{Ca}=0.50$, the strontium dissolved in the phase reaches saturation, while the strontium solid solubility limit of the phase is between 0.67 and 0.75, and beyond this limit the crystal structure is greatly distorted.

1. Introduction

Bismuth-based superconductors in the series $\text{Bi}_2\text{Sr}_2\text{Ca}_{n-1}\text{Cu}_n\text{O}_8$ [1, 2] are members of the structural family that includes thallium-containing compositions with the highest values of T_c yet reported. Unlike the thallium-system, the nominal three-layer bismuth analogue, $\text{Bi}_2\text{Sr}_2\text{Ca}_2\text{Cu}_3\text{O}_8$ (2223) is still difficult to synthesize in its pure form, for the formation of 2223 is a much slower process taking place in a very limited temperature range [3, 4]. It is therefore desirable to discover more about the reaction process in the BSCCO system with the goal of understanding the formation reaction of its superconducting phases. Once the reaction path has been found it can be modified by avoiding or promoting certain phases using binary or ternary oxide components as starting materials. Thus, the stability range of desired superconducting phases can be enlarged or their formation accelerated.

Previously, we studied systematically [5] the reaction process of the BSCCO system and found out that $\text{Bi}_2\text{Sr}_2\text{CaCu}_2\text{O}_8$ (2212) is formed by the reaction of a Bi–Sr–Ca–O ternary unknown intermediate phase, together with CuO, SrO and CaO. This intermediate phase is a solid solution of Bi–Ca–O and Bi–Sr–O, and called interphase for short. From the results, we presented a new two-step method to prepare the 2212 phase through the presynthesized interphase. Using this method, it is easy to adjust the strontium solid solubility of 2212, which affects its electromagnetic properties greatly [5, 6]. Thus, it is necessary to study the solid solubility of the interphase. In the present paper, the formation, composition, and solid solution structure of the interphase is reported and the crystallography data of the phase are given.

2. Experimental procedure

Samples were prepared by (1) weighing and mixing analytically pure Bi_2O_3 , SrCO_3 and CaCO_3 in the desired proportions as shown in Table I, (2) grinding in an agate ball mill for 3 h, and (3) pressing the mixed powders into pellets. The pellets were sintered under the conditions listed in Table I. Sintering temperatures were selected according to the differential thermal analysis (DTA) curves of the mixed powders.

The diffraction data were collected using a D/max-III B type diffractometer using CuK_α radiation at 40 kV and 20 mA. The scanning speed is $1^\circ 2\theta \text{ min}^{-1}$. The resulting 2θ is rectified at $5^\circ\text{--}25^\circ$ and $25^\circ\text{--}55^\circ$ using tetradecanol-[1] ($\text{CH}_3(\text{CH}_2)_{12}\text{CH}_2\text{OH}$) and silicon as standard materials, respectively. Unit-cell parameters were calculated by using the program TREOR [7] and refined by least squares analysis. The cell parameters should be regarded as preliminary. Either single-crystal X-ray or electron diffraction studies will be required to refine the structure of this compound. Morphology was observed and microarea composition was analysed using a Hitachi S-570 scanning electron microscope (SEM) with energy-dispersive X-ray spectroscopy (EDXS).

3. Results and discussion

3.1. The formation and the composition of the interphase

Fig. 1 shows the XRD spectra of Bi–Ca–O and Bi–Sr–Ca–O binary and ternary samples. Except for the diffraction peaks of formed $\text{Ca}_7\text{Bi}_{10}\text{O}_{22}$ [8, 9], unreacted remaining SrCO_3 and a small amount of free CaO, the rest correspond well with each other, but they cannot conform to the already known diffraction

TABLE I Sample compositions and sintering conditions

Composition	x, y	Sintering conditions
$\text{BiSr}_y\text{CaO}_{2.50+y}$	0.00, 0.25, 1.00	730 °C/5 h; 815 °C/5 h, quenched in liquid nitrogen
$\text{BiCa}_y\text{O}_{1.50+y}$	0.50, 0.75, 1.00 1.25, 1.50, 1.75	800 °C/15 h, quenched in air
$\text{BiSr}_x\text{Ca}_{1-x}\text{O}_{2.50}$	0.00, 0.25, 0.33 0.50, 0.67, 0.75	800–830 °C/24 h, quenched in air

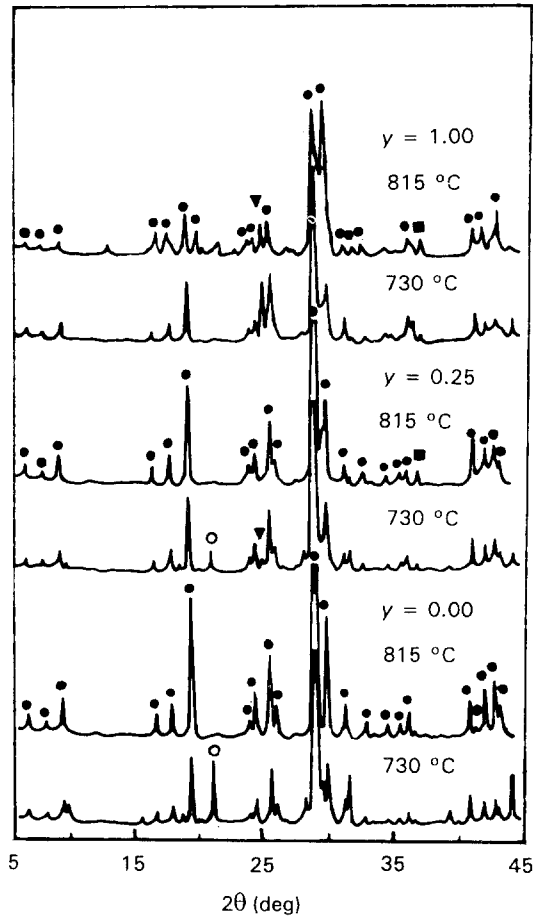


Figure 1 XRD patterns of the $\text{BiSr}_y\text{CaO}_{2.50+y}$ ($y = 0.00, 0.25, 1.00$) samples sintered at 730 °C or 815 °C for 5 h. (●) Interphase, (■) CaO, (○) $\text{Ca}_7\text{Bi}_{10}\text{O}_{22}$, (▼) SrCO_3 .

spectra of chemical compounds in the system, which indicates that the same unknown phase may be formed in these samples, i.e. what we call interphase [5]. Now it has been determined that 2212 superconducting phase is formed through the interphase [5], which has yet to be indexed.

The Bi–Ca–O binary sample sintered at 730 °C mainly includes interphase and a small amount of $\text{Ca}_7\text{Bi}_{10}\text{O}_{22}$; with rising sintering temperature, the former increases, the latter decreases. In Bi–Sr–Ca–O ternary samples, at the same sintering temperature, the amount of $\text{Ca}_7\text{Bi}_{10}\text{O}_{22}$ is much smaller. For the samples sintered at 815 °C in both systems, $\text{Ca}_7\text{Bi}_{10}\text{O}_{22}$ disappears, only interphase, a small amount of free CaO and the remaining SrCO_3 being present. Therefore, it is reasonable to think that Bi–Ca–O binary interphase is formed by the trans-

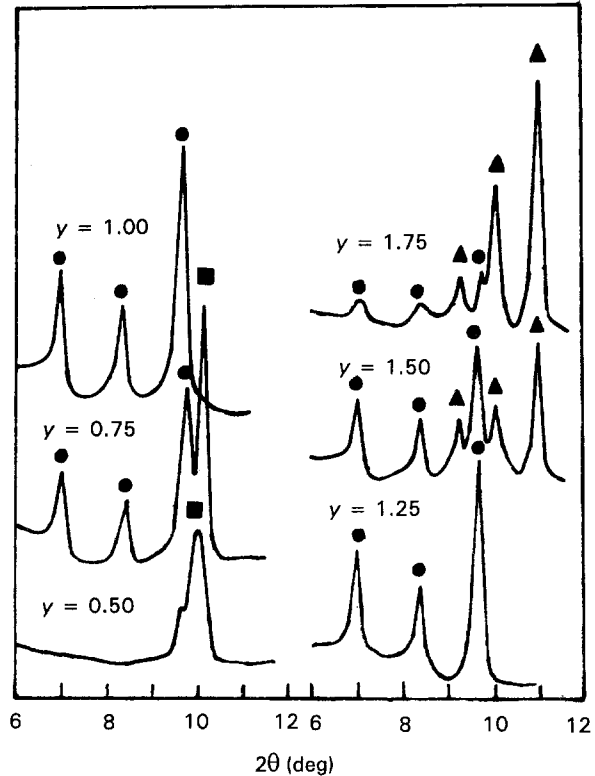


Figure 2 XRD patterns (low-angle part) of the $\text{BiCa}_y\text{O}_{1.50+y}$ ($y = 0.50, 0.75, 1.00, 1.25, 1.50, 1.75$) samples sintered at 800 °C for 15 h. (●) Interphase, (■) $\text{Ca}_7\text{Bi}_{10}\text{O}_{22}$, (▲) $\text{Ca}_7\text{Bi}_6\text{O}_{16}$.

formation of $\text{Ca}_7\text{Bi}_{10}\text{O}_{22}$. The existence of strontium is favourable to the transformation to interphase containing strontium. Whether or not it is a binary or ternary system, mono-interphase can be obtained through the adjustment of compositions and sintering conditions.

The XRD patterns (low-angle part) of the samples with nominal composition $\text{BiCa}_y\text{O}_{1.50+y}$ ($y = 0.50–1.75$) are shown in Fig. 2. For $y = 0.50$, the lower calcium sample, no interphase but many miscellaneous phases and some $\text{Ca}_7\text{Bi}_{10}\text{O}_{22}$ are formed. With the increasing y , interphase begins to emerge, the amount increasing accordingly and reaching its highest value for $y = 1.00$; but with the further increase in y , the amount of interphase decreases; if $y > 1.25$, it decreases dramatically and meantime $\text{Ca}_7\text{Bi}_6\text{O}_{16}$ [8, 9] is formed. Only interphase is found in the $y = 1.00$ sample, while in the $y = 1.25$ sample, there is not only interphase but also some free CaO. Therefore, the ratio, y , of calcium to bismuth is important in the formation of binary mono-interphase, and the most suitable composition is $y = 1.00$. The microarea

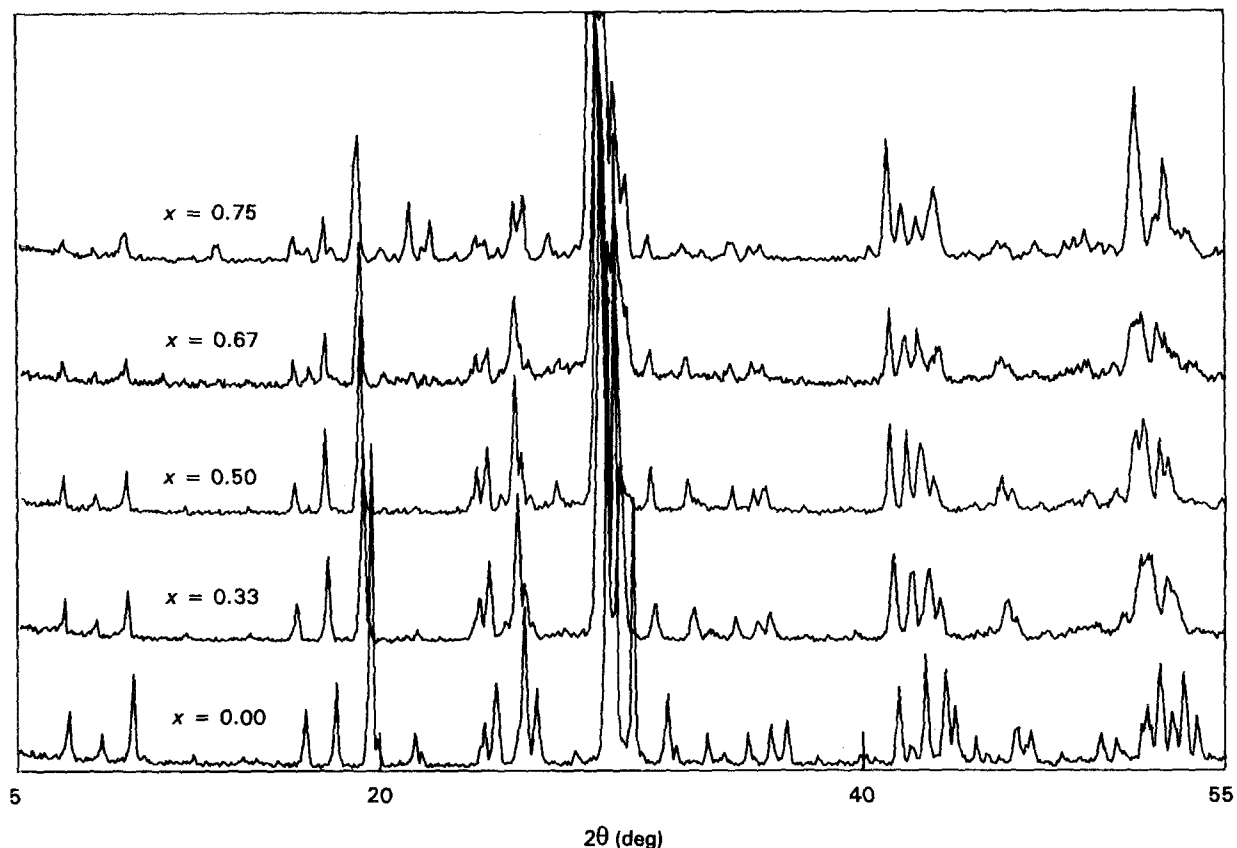


Figure 3 XRD patterns of $\text{BiSr}_x\text{Ca}_{1-x}\text{O}_{2.50}$ with different strontium contents.

TABLE II X-ray powder diffraction data of $\text{BiCaO}_{2.50}$

hkl	d_{obs} (nm)	d_{cal} (nm)	I/I_0	hkl	d_{obs} (nm)	d_{cal} (nm)	I/I_0
10 $\bar{1}$	1.234	1.240	9	60 $\bar{4}$	0.2543	0.2546	6
101	1.036	1.041	6	50 $\bar{5}$	0.2479	0.2481	7
200	0.9000	0.9035	15	30 $\bar{5}$	0.2437	0.2439	8
002/00 $\bar{2}$	0.7202	0.7218	3	21 $\bar{5}$	0.2357	0.2353	2
20 $\bar{2}$	0.6163	0.6204	2	800	0.2260	0.2259	2
30 $\bar{1}$	0.5941	0.5948	2	71 $\bar{3}$	0.2244	0.2240	2
301	0.5227	0.5237	9	801	0.2175	0.2173	13
10 $\bar{3}$	0.4860	0.4870	14	024/02 $\bar{4}$	0.2150	0.2153	4
400	0.4510	0.4518	52	70 $\bar{5}$	0.2120	0.2121	18
103	0.4449	0.4457	5	41 $\bar{5}$	0.2081	0.2081	16
30 $\bar{3}$	0.4134	0.4136	6	007/00 $\bar{7}$	0.2063	0.2062	10
112	0.4085	0.4092	3	51 $\bar{6}$	0.2025	0.2028	5
31 $\bar{2}$	0.3690	0.3694	4	52 $\bar{2}$	0.2008	0.2007	3
40 $\bar{3}$	0.3635	0.3632	7	80 $\bar{5}$	0.1959	0.1956	6
20 $\bar{4}$	0.3583	0.3578	14	621	0.1953	0.1953	7
303	0.3468	0.3470	5	207	0.1933	0.1937	6
113	0.3423	0.3429	26	31 $\bar{7}$	0.1928	0.1929	4
501	0.3358	0.3367	13	41 $\bar{7}$	0.1886	0.1888	3
204	0.3170	0.3163	3	10 $\bar{8}$	0.1827	0.1826	6
51 $\bar{1}$	0.3035	0.3025	80	008/00 $\bar{8}$	0.1805	0.1804	5
600	0.3007	0.3012	100	70 $\bar{7}$	0.1772	0.1772	7
10 $\bar{5}$	0.2929	0.2933	43	407	0.1763	0.1761	10
30 $\bar{5}$	0.2801	0.2805	12	903	0.1748	0.1746	17
105	0.2771	0.2775	4	21 $\bar{8}$	0.1732	0.1735	9
503	0.2668	0.2670	6	208	0.1714	0.1712	15
205	0.2616	0.2618	3	10 $\bar{1}\bar{3}$	0.1702	0.1706	8

composition analysis of the interphase by EDXS gives $y = 1.07$, so the composition of Bi–Ca–O binary interphase is very close to $\text{BiCaO}_{2.50}$.

Fig. 3 shows the XRD patterns of $\text{BiSr}_x\text{Ca}_{1-x}\text{O}_{2.50}$ samples with different strontium contents. The pat-

terns involve five groups of relatively concentrated characteristic peaks at about $2\theta = 6^\circ\text{--}10^\circ$, $16^\circ\text{--}20^\circ$, $23^\circ\text{--}27^\circ$, $41^\circ\text{--}44^\circ$ and $51^\circ\text{--}53^\circ$, respectively. With x varying between 0.00 and 0.67, almost all the peaks in the patterns correspond with one another, and when x

TABLE III X-ray powder diffraction data of $\text{BiSr}_{0.50}\text{Ca}_{0.50}\text{O}_{2.50}$

hkl	d_{obs} (nm)	d_{cal} (nm)	I/I_0	hkl	d_{obs} (nm)	d_{cal} (nm)	I/I_0
10 $\bar{1}$	1.264	1.261	7	20 $\bar{5}$	0.2961	0.2958	6
101	1.063	1.062	4	005/00 $\bar{5}$	0.2946	0.2945	4
200	0.9210	0.9188	7	30 $\bar{5}$	0.2857	0.2855	8
002/00 $\bar{2}$	0.7366	0.7362	2	503	0.2727	0.2723	6
30 $\bar{1}$	0.6062	0.6041	2	60 $\bar{4}$	0.2587	0.2586	5
301	0.5342	0.5336	5	50 $\bar{5}$	0.2525	0.2522	4
30 $\bar{2}$	0.5175	0.5172	2	305	0.2497	0.2490	5
10 $\bar{3}$	0.4971	0.4962	13	215	0.2390	0.2390	2
400	0.4602	0.4594	30	514	0.2190	0.2189	14
112	0.4117	0.4115	2	70 $\bar{5}$	0.2156	0.2155	13
31 $\bar{2}$	0.3723	0.3716	3	10 $\bar{7}$	0.2131	0.2132	10
40 $\bar{3}$	0.3691	0.3690	8	415	0.2117	0.2115	7
20 $\bar{4}$	0.3648	0.3643	6	007/00 $\bar{7}$	0.2102	0.2103	6
402	0.3625	0.3624	11	216	0.2096	0.2092	5
303	0.3549	0.3541	4	207	0.1978	0.1977	6
113	0.3466	0.3463	21	605	0.1961	0.1959	4
501	0.3433	0.3428	10	008/00 $\bar{8}$	0.1842	0.1841	4
312	0.3382	0.3373	4	70 $\bar{7}$	0.1802	0.1802	4
204	0.3237	0.3228	6	903	0.1778	0.1778	13
600	0.3072	0.3063	100	21 $\bar{8}$	0.1767	0.1764	7
51 $\bar{1}$	0.3055	0.3053	62	208	0.1747	0.1747	12
10 $\bar{5}$	0.2993	0.2990	34	10 $\bar{13}$	0.1730	0.1730	6

TABLE IV Lattice parameters of $\text{BiSr}_x\text{Ca}_{1-x}\text{O}_{2.50}$

$\text{BiSr}_x\text{Ca}_{1-x}\text{O}_{2.50}$	a (nm)	b (nm)	c (nm)	β (deg)	V (nm ³)
$\text{BiCaO}_{2.50}$	1.8363	0.5366	1.4670	100.26	1.42241
$\text{BiSr}_{0.25}\text{Ca}_{0.75}\text{O}_{2.50}$	1.8563	0.5356	1.4820	99.95	1.45129
$\text{BiSr}_{0.33}\text{Ca}_{0.67}\text{O}_{2.50}$	1.8588	0.5345	1.4869	99.96	1.45501
$\text{BiSr}_{0.50}\text{Ca}_{0.50}\text{O}_{2.50}$	1.8661	0.5341	1.4952	100.03	1.46747
$\text{BiSr}_{0.67}\text{Ca}_{0.33}\text{O}_{2.50}$	1.8676	0.5330	1.4983	100.04	1.46861
$\text{BiSr}_{0.75}\text{Ca}_{0.25}\text{O}_{2.50}$	1.8761	0.5331	1.5014	100.08	1.47845

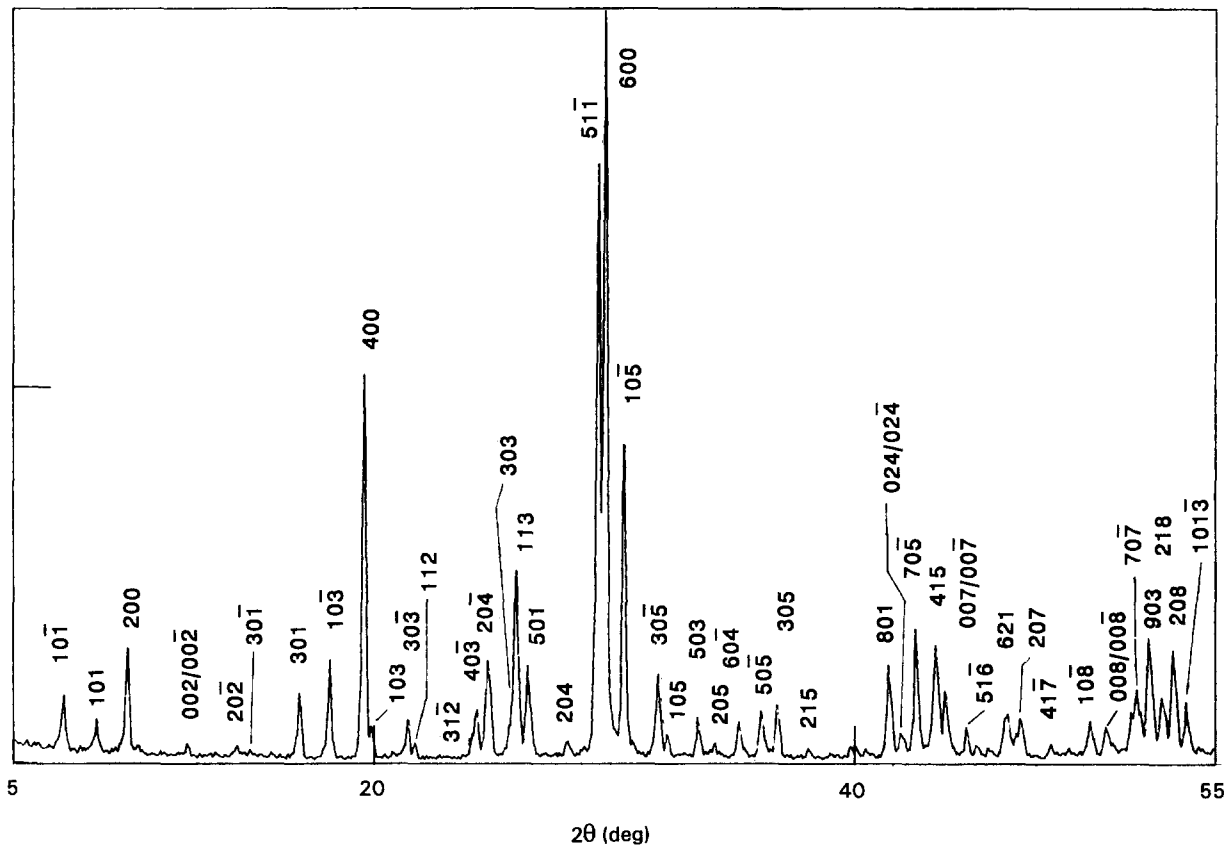


Figure 4 Indexed XRD pattern of $\text{BiCaO}_{2.50}$.

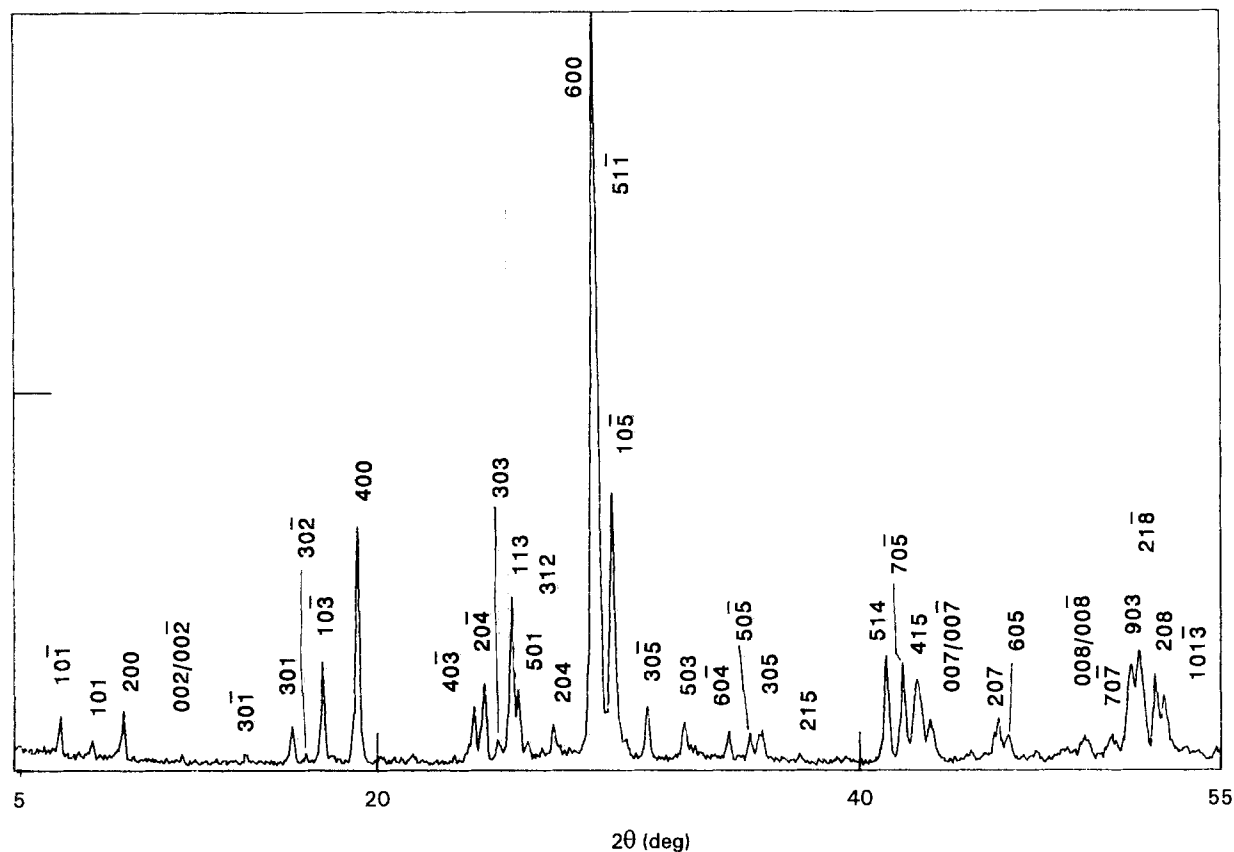


Figure 5 Indexed XRD pattern of $\text{BiSr}_{0.50}\text{Ca}_{0.50}\text{O}_{2.50}$.

$x = 0.75$, the five groups of characteristic peaks still exist but some apparently new peaks appear. All diffraction peaks for every sample can be indexed as interphase (see below), that is, the samples only involve interphase. Meanwhile, all 2θ values shift towards low-angle with increasing x . Thus, the interphase is a solid solution of Bi–Ca–O and Bi–Sr–O; its composition should be $\text{BiSr}_x\text{Ca}_{1-x}\text{O}_{2.50}$. With x increasing up to 0.75, the structural frame of $\text{BiSr}_x\text{Ca}_{1-x}\text{O}_{2.50}$ remains unchanged.

3.2. The solid solution structure of $\text{BiSr}_x\text{Ca}_{1-x}\text{O}_{2.50}$

Previously [6], we have preliminarily indexed the $\text{BiCaO}_{2.50}$ binary interphase. However, our present work on the solid-solution structure of $\text{BiSr}_x\text{Ca}_{1-x}\text{O}_{2.50}$ has found that the previous crystallography data of $\text{BiCaO}_{2.50}$ cannot be applied to $\text{BiSr}_x\text{Ca}_{1-x}\text{O}_{2.50}$ when $x \neq 0$. $\text{BiSr}_x\text{Ca}_{1-x}\text{O}_{2.50}$ is strontium and calcium solid solution. The structures of $\text{BiSr}_x\text{Ca}_{1-x}\text{O}_{2.50}$ should maintain consistency. Thus the previous data of $\text{BiCaO}_{2.50}$ should be revised. The structures of $\text{BiSr}_x\text{Ca}_{1-x}\text{O}_{2.50}$ is now discussed in detail.

The diffraction lines of $\text{BiSr}_x\text{Ca}_{1-x}\text{O}_{2.50}$ were indexed using Werner's TREOR program [7] and the indexed powder diffraction data are listed in Tables II and III, and the X-ray powder diffraction patterns are illustrated in Figs 4 and 5. The crystals of $\text{BiSr}_x\text{Ca}_{1-x}\text{O}_{2.50}$ have a monoclinic unit cell with space group $P1m1$ or $P12/m1$ and the unit cell parameters are listed in Table IV.

The calculated interplanar distances, d_{cal} , agree well with the observed ones, d_{obs} , when x varies between 0.00 and 0.67 (see Tables I and II). But when $x = 0.75$, the deviations between d_{cal} and d_{obs} for some peaks are somewhat large. The reason for this is that excessive strontium solid solubility makes its crystal structure distort greatly and its diffraction peaks broaden, which makes it difficult to obtain accurate 2θ values. Fig. 6 shows the variation of a , b , c and the volume, V , of the unit cell with strontium solid solubility, x . The a , b , c and V vary linearly with the increasing strontium solid solubility, x , from 0.00 up to 0.33, and gradually tend to saturate at about $x = 0.50$. But the a and V increase suddenly at about $x = 0.67$. Therefore, we can infer that the strontium solid solubility limit of $\text{BiSr}_x\text{Ca}_{1-x}\text{O}_{2.50}$ is between 0.67 and 0.75, and beyond this limit the crystal structure is greatly distorted.

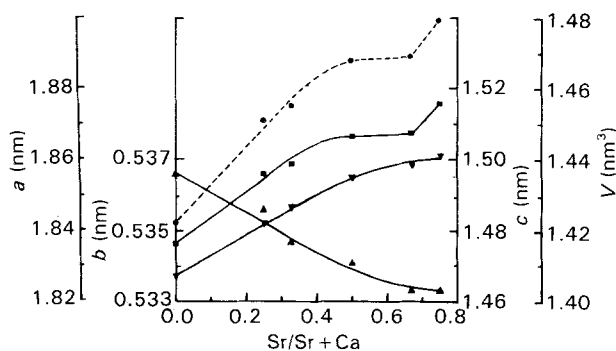


Figure 6 Lattice parameters (■) a , (▼) b , (▲) c and (●) V of $\text{BiSr}_x\text{Ca}_{1-x}\text{O}_{2.50}$ dependence of strontium solid solubility $x = \text{Sr}/(\text{Sr} + \text{Ca})$.

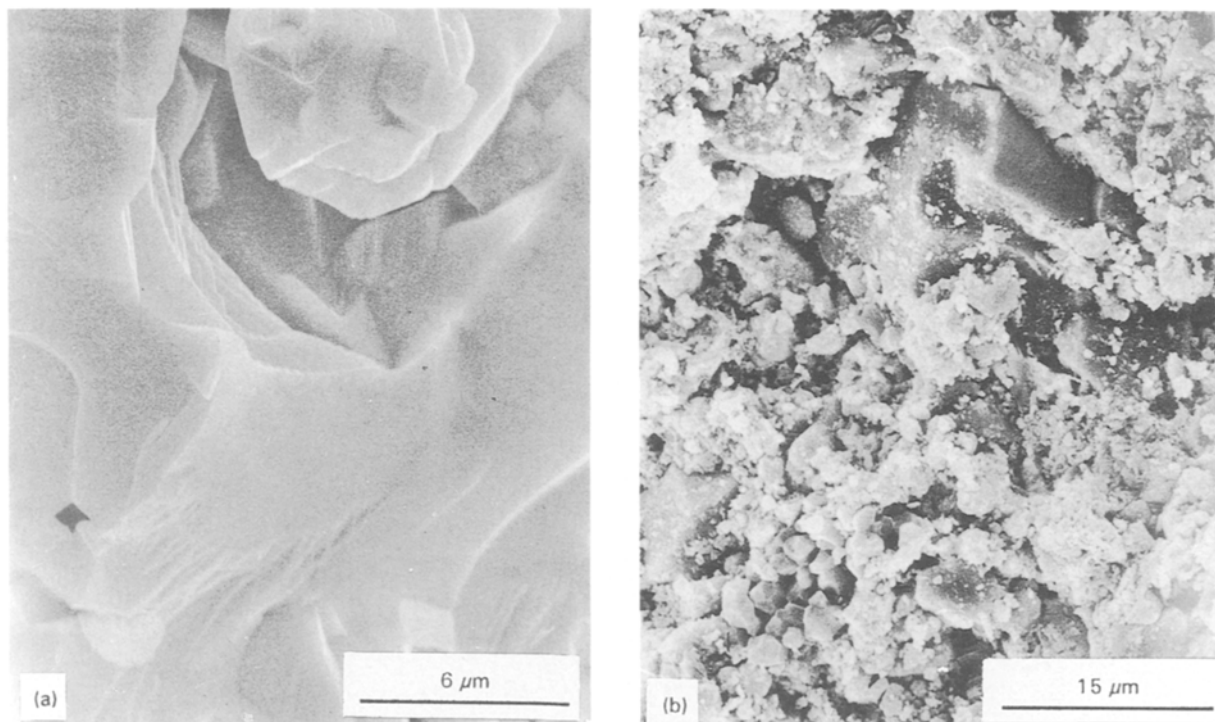


Figure 7 Scanning electron micrographs of interphase with different strontium solid solubilities. (a) $x = 0.50$, (b) $x = 0.75$.

Scanning electron micrographs of the interphase with different strontium solid solubility are shown in Fig. 7 and reveal that plate-like morphology for lower strontium interphase ($x = 0.50$) becomes a powdery morphology for high strontium interphase ($x = 0.75$), which apparently results from the structure distortion of the interphase containing excessive strontium.

4. Conclusion

$\text{BiSr}_x\text{Ca}_{1-x}\text{O}_{2.50}$ is the solid solution of Bi–Ca–O and Bi–Sr–O. The strontium dissolved in the phase reaches saturation when its solid solubility $x = \text{Sr}/\text{Sr} + \text{Ca} = 0.50$, while the strontium solid solubility limit of the phase is between 0.67 and 0.75. The crystallographic data of $\text{BiSr}_x\text{Ca}_{1-x}\text{O}_{2.50}$ are also given.

References

1. H. MAEDA, T. TANAKA, M. FUKUTOMI and T. ASANO, *Jpn J. Appl. Phys.* **27** (1988) L209.

2. A. OTA, K. OHBA, A. ISHIDA, A. KIRIHIGASHI, K. IWASAKI and H. KUWAJIMA, *ibid.* **28** (1989) L1171.
3. K. SONG, H. LIN, S. DON and C. SORRELL, *J. Am. Ceram. Soc.* **73** (1990) 1771.
4. B. SEEBACHER, B. JOBST and G. ZORN, in "Proceedings of the 1st European Ceramic Society Conference", Maastricht, edited by G. de With, R. A. Terpstra and R. Metselaar, *Euro-Ceramics 2* (1989) p. 2456.
5. GUOHONG XIONG, MINQUAN WANG, XIANPING FAN and XIAOMING TANG, *Appl. Phys. A* **56** (2) (1993) 99.
6. MINQUAN WANG, GUOHONG XIONG and XIAODAN FANG, *J. Chinese Ceram. Soc.* **20** (1) (1992) 29.
7. P. E. WERNER, *J. Appl. Crystallogr.* **9** (1976) 216.
8. P. CONFLANT, J. C. BOVIN and D. J. THOMAS, *J. Solid State Chem.* **18** (1976) 1333.
9. P. CONFLANT, J. C. BOVIN and G. TRIDOT, *C. R. Hebd. Seances Acad. Sci.* **279** (1974) 457.

Received 13 October 1993
and accepted 16 May 1994